Contribution of complex stapes motion to cochlea activation

Eiber, A ; Huber, A M ; Lauxmann, M ; Chatzimichalis, M ; Sequeira, D ; Sim, J H

Abstract: Classic theories of hearing have considered only a translational component (piston-like component) of the stapes motion as being the effective stimulus for cochlear activation and thus the sensation of hearing. Our previous study [Huber, A.M., Sequeira, D., Breuninger, C., Eiber, A., 2008. The effects of complex stapes motion on the response of the cochlea. Otol. Neurotol. 29: 1187–1192.] qualitatively showed that rotational components around the long and short axes of the footplate (rocking-like components) lead to cochlear activation as well. In this study, the contribution of the piston-like and rocking-like components of the stapes motion to cochlea activation was quantitatively investigated with measurements in live guinea pigs and a related mathematical description. The isolated stapes in anesthetized guinea pigs was stimulated by a three-axis piezoelectric actuator, and 3-D motions of the stapes and compound action potential (CAP) of the cochlea were measured simultaneously. The measured values were used to fit a hypothesis of the CAP as a linear combination of the logarithms of the piston-like and rocking-like components. Both the piston-like and rocking-like components activate cochlear responses when they exceed certain thresholds. These thresholds as well as the relation between CAP and intensity of the motion component were different for piston-like and rocking-like components. The threshold was found to be higher and the sensitivity lower for the rocking-like component than the corresponding values for the piston-like component. The influence of the rocking-like component was secondary in cases of piston-dominant motions of the stapes although it may become significant for low amplitudes of the piston-like component.

DOI: https://doi.org/10.1016/j.heares.2011.11.008

CONTRIBUTION OF COMPLEX STAPES MOTION TO COCHLEA ACTIVATION

Albrecht Eiber[1], Alexander M. Huber[2], Michael Lauxmann[1], Michail Chatzimichalis[2], Damien Sequeira[2], and Jae Hoon Sim[2,*]

[1]*University of Stuttgart,* [2]*University Hospital Zurich,*

*Corresponding author:

Name: Jae Hoon Sim

Address: Department of Otorhinolaryngology, Head and Neck Surgery
University Hospital Zurich, Frauenklinikstrasse 24, 8091 Zürich,
SWITZERLAND

Email: JaeHoon.Sim@usz.ch

Tel. No.: +41 44 255 36 80

Fax No.: +41 44 255 41 64

Abstract

Classic theories of hearing have considered only a translational component (piston-like component) of the stapes motion as being the effective stimulus for cochlear activation and thus the sensation of hearing. Our previous study (Huber et al. 2008) qualitatively showed that rotational components around the long and short axes of the footplate (rocking-like components) lead to cochlear activation as well. In this study, the contribution of the piston-like and rocking-like components of the stapes motion to cochlea activation was quantitatively investigated with measurements in live guinea pigs and a related mathematical description. The isolated stapes in anesthetized guinea pigs was stimulated by a three-axis piezoelectric actuator, and 3-D motions of the stapes and compound action potential (CAP) of the cochlea were measured simultaneously. The measured values were used to fit a hypothesis of the CAP as a linear combination of the logarithms of the piston-like and rocking-like components. Both the piston-like and rocking-like components activate cochlear responses when they exceed certain thresholds. These thresholds as well as the relation between CAP and intensity of the motion component were different for piston-like and rocking-like components. The threshold was found to be higher and the sensitivity lower for the rocking-like component than the corresponding values for the piston-like component. The influence of the rocking-like component was secondary in cases of piston-dominant motions of the stapes although it may become significant for low amplitudes of the piston-like component.

Keywords: Auditory mechanics; Cochlear mechanics; Cochlear physiology ; Compound action potential (CAP); Guinea pig; Laser Doppler interferometry (LDI); Piston-like component; Rocking-like component; Stapes

1. Introduction

Previous measurements have revealed that the physiological motions of the stapes in human and other mammals include more than only piston-like movement. Georg von Békésy (1960) described the movement of the stapes in human temporal bones with drained cochleae as rotating around an axis near the posterior edge of the footplate, so that the anterior portion of the footplate had larger displacements than the posterior portion. Kirikae (1960) performed similar experiments and concluded that the vibration pattern of the stapes footplate was a combination of three movements: piston-like, hinged rotation around a posterior axis, and rotation around the long axis of the footplate. Both authors used temporal bones (TBs) with drained cochleae in their studies. Therefore, their measurements did not represent physiologic motions, since it has been shown in more recent experiments that movement patterns of the stapes footplate change when the cochlea is drained (Gyo et al. 1987; Hato et al. 2003). Gundersen (1971) showed that a piston-like motion pattern was preserved up to 2 kHz, but movements of the stapes in an "uneven manner" appeared at higher frequencies. He used a "contacting" measurement technique that may have influenced the vibration modes. Recent developments in measurement techniques and methods have shown complex modes of the stapes motions more clearly. Using a video measuring system, Gyo et al. (1987) observed predominant piston-like movements only at low frequencies and complex movements at higher frequencies. Other studies in human and animals are in accordance with these findings (Asai et al. 1999; Decraemer & Khanna 1999; Voss et al. 2000; Hato et al. 2003; Stenfelt and Goode 2005; Decraemer et al. 2007; Ravicz et al. 2008; Sim et al. 2010a). Some previous studies, assuming that the annular ring of the stapes restricts motions of the stapes footplate in the plane of the footplate, considered piston-like motions (i.e., the translational motion in a direction perpendicular to the stapes footplate) and two rocking-like motions of the stapes (i.e., the two rotational motions along the long and short axes of the footplate) as primary motion components of the mammal stapes. While it has not been proven that other motions of the stapes are insignificant, we shall assume, as have others (Hato et al. 2003; Sim et al. 2010a), that the piston-like motion and the two rocking motions dominate stapes mechanics.

The effects of the rocking-like motions on hearing in humans and other mammals are still controversial. Decraemer et al. (2007) measured three-dimensional motions of the stapes and scala-vestibuli pressure in gerbil ears and concluded that the scala-vestibuli pressure was well correlated with the piston-like component of the stapes motion. Rochefoucauld et al. (2008) observed that scala vestibuli pressure followed the piston-like component of the stapes motion with high fidelity, reinforcing their previous finding that the piston-like motion of the

stapes was the main stimulus to the cochlea. Many previous models of the cochlea ignore the effects of the rocking-like motions because these motions did not produce net volume displacement on the oval window, thus were believed to have negligible effects on hearing mechanisms (Kolston and Ashmore 1996; Dodson 2001; Lim and Steele 2002: Pozrikidis 2008). However, measurement of the effects of the rocking-like motions has been limited because it is difficult to separate the relatively small effects of the rocking-like motions from the effects of the piston-like motions under physiological conditions. In our recent study (Huber et al. 2008), the rocking-like motions of the stapes in live guinea pigs were enhanced by direct stimulation on the stapes with a mechanical actuator, and clear effects of the rocking-like motions on compound action potential (CAP) were observed. The CAP, which is a variation in cochlea potential due to the synchronous discharge of a large number of fibers in the auditory nerve, is known to be best elicited by short stimuli and reliable up to near threshold levels, and have nonlinear response characteristics (Dallos 1973; Schmiedt 1979).

There have also been reported pathological cases that suggest cochlear activation by the rocking-like motions of the stapes. In patients with round window atresia, in which the deformable round window membrane was covered by solid bone and thus considerable amounts of the pure piston-like motions could not be generated, a mixed hearing loss with air-bone gaps between 15 and 30 dB over a frequency range of 0.25 to 8 kHz were recorded, instead of a total hearing loss (Ombredanne 1968; Richards 1981, Linder et al. 2003). However, hearing in such cases cannot be simply considered as the effects of the rocking-like motions because the possibility of fluid flow through a potential third window still exists (Shera and Zweig 1992).

The goal of this study was to confirm the effects of the rocking-like components of the stapes motion on the CAP as determined in our previous study (Huber et al. 2008) and to correlate the piston-like and rocking-like components of the stapes motions quantitatively to their corresponding cochlear electro-physiological responses through measurements in live guinea pigs. A simple mathematical description of the CAP as a linear combination of logarithms of the piston-like and rocking-like components was introduced. In this study, the stapes was stimulated by translational motions of a mechanical actuator that had a point-like contact to the stapes head. Since only forces were applied at this pivot point on the stapes head quite apart from the footplate, the in-plane motions of the footplate at the oval window were considered to play a secondary role.

2. Methods

2.1. Animal Preparation and Experimental Setup

Ethical permission for the study was obtained from the local veterinary authority according to national animal protection laws (permission no. 25/2008).

Thirteen pathogen-free female guinea pigs of the same age, weight class, and family were used for the experiments. Three animals among the total of thirteen died during preparation or at the beginning of the measurements without sufficient sets of measurements being obtained. In another four, the CAP signals were not detected clearly due to technical difficulties, and their results were deleted from the data set. As a consequence, measurements in the remaining six guinea pigs were analyzed for this study.

General anesthesia with ketamine (35 mg/kg, i.m.) and xylazine (5 mg/kg, i.m.) was applied, a posterior opening of the bulla was made, and the incudo-stapedial joint was dissected for mechanical stimulation on the stapes head. The head of the animals was fixed with a custom-made head holder, and the head holder was mounted to a custom-made aluminum test stand. A 3-D laser Doppler interferometer (LDI) system (CLV-3000, CLV-3D, Polytec, Waldbronn, Germany) and a three-axis piezoelectric actuator were also mounted to the test stand. The animal holder and the stimulator were adjustable by micromanipulators and goniometers (Breuninger 2008). A surgical microscope was used to align the long axis of the stapes footplate along the direction of the "directional indicator" on the head holder, and the head-holder was placed in the test stand such that the long and short axes of the footplate were parallel and perpendicular to the three axes of the test stand (Sim et al. 2010b). To measure the CAP as a response of the cochlea, a custom-made silver-ball electrode was placed in the round window niche. Detailed procedures concerning the animal handling and experimental setups were provided in our previous study (Huber et al. 2008).

2.2. Mechanical Stimulation of the Stapes and Measurements

Details about mechanical excitation and measurement procedures used in this study were described in our previous publications (Eiber et al. 2007; Breuninger 2008, Huber et al. 2008; Sim et al. 2010b).

A custom-made three-axis piezoelectric actuator was used to stimulate the surgically exposed stapes of the guinea pig. A firm contact between the needle tip of the actuator and the stapes head was obtained through a monofilament nylon thread (0.03-mm diameter, 9-0 Nylon, S&T AG, Switzerland) guided through the needle tied around the stapes head. Clicks with a duration of 0.4 ms were used as the excitation signal. First, the appropriate electric signals for the three axes of the actuator needed to obtain the desired motions of the stapes

were determined. Then, the stimulation was performed such that the magnitude ratio of the rocking-like component to the piston-like component in the stapes motion (defined as k in section 2.4) had several different values. Depending on the magnitude ratio k, the stapes motions were piston-like dominant ($k<<1$), rocking-like dominant ($k>>1$), or of mixed modes. Stimulation modes with different values of k were applied to each of the animals, and measurements were done with several intensity levels of stimulation for each k value.

With stimulation by the three-axis piezoelectric actuator, stapes motions and the CAP generated from the cochlea were simultaneously monitored. First, the 3-D laser Doppler interferometer (LDI) system with three separate laser beams was used to measure the 3-D motion components of a point on the stapes head. Then, the 3-D motion components at that point were decomposed into a piston-like and two rocking-like components of the stapes motions using kinematics of the rigid body motion. With the assumption that motions of the stapes other than the piston-like and two rocking-like motions of the stapes, as defined in this study, are negligible, displacements $d_x = h\gamma$ and $d_z = -h\alpha$ at the stapes head represent the rocking-like components around the short and the long axis of the footplate, and displacement d_y represents the piston-like components of the stapes motion (Fig.1). The electric signal of the cochlea measured through the silver-ball electrode was processed by a differential amplifier (Dagan Corp., Minneapolis, MN, USA). All of the amplified signals were recorded with a sampling frequency of 51.2 kHz.

To confirm a perfect contact between the stapes and the actuator needle at their interface (i.e., no relative motion), the measurement was repeated with stimuli in the opposite direction. In these measurements, the stapes motion and CAP showed almost the same magnitude (only direction of the stapes motion was opposite). Otherwise, the contact between the stapes and the needle was checked and rearranged.

2.3. Data Processing

Each measurement was repeated 200 times. The recorded data were processed in the narrowed time window (0 to 2 ms in the measured stapes motion and 0 to 4 ms in the measured CAP), and constant and linear trends were removed using a built-in function 'detrend' provided by Matlab (The Mathworks Inc). The different sizes of time windows between the measured stapes motion and the measured CAP were due to time delays between the two signals (CAP signals usually had time delays of 0.7 to 1.5 ms from the stapes-motion signals). Corrupted data showing large deviations from other data were excluded and the

remaining data sets averaged. Figure 2 displays the measured stapes motions (A) and CAP values (B) before and after the offset and trends were eliminated.

When the desired motion form was not achieved (e.g., time shift, distorted motion form), the corresponding data were removed. The measured CAP values usually showed significant reduction near the animal's death, which was usually six-to-eight hours from the anesthesia. These data were also removed. After the data were processed, the peak values in CAP and velocity data with two opposite directions of stimuli (described as 'plus' and 'minus' in Fig. 2B) were obtained for the corresponding signals. The magnitudes of these two peak values with the 'plus' and 'minus' directions of stimuli were averaged.

2.4. Mathematical Description of Relation between Stapes Motion and CAP

It is presumed that the contribution of the stapes motion components to cochlear activation corresponds to their contribution to hearing. In this study, cochlear activation was monitored by measuring the compound action potential (CAP). It is assumed that the total CAP has two independent components: a contribution by the piston-like component and separately by the rocking-like component

$$CAP = CAP_p + CAP_r, \tag{1}$$

where CAP_p and CAP_r indicate CAP values by piston-like and rocking-like components of the stapes motion, respectively. In relating each of the two CAP components to the corresponding motion component of the stapes, a linear relationship between the logarithm of the motion component and CAP components was used based on the results of our previous study (Huber et al. 2008)

$$CAP_p = \begin{cases} a_p \log\left(|d_p| / |d_p|_{th}\right) & for \quad |d_p| \geq |d_p|_{th} \\ 0 & for \quad |d_p| \leq |d_p|_{th} \end{cases}, \tag{2}$$

$$CAP_r = \begin{cases} a_r \log\left(|d_r| / |d_r|_{th}\right) & for \quad |d_r| \geq |d_r|_{th} \\ 0 & for \quad |d_r| \leq |d_r|_{th} \end{cases}, \tag{3}$$

where $|d_p|$ and $|d_r|$ represent magnitudes of the piston-like and rocking-like displacements, and $|d_p|_{th}$ and $|d_r|_{th}$ represent the minimum magnitude of the displacements to produce CAP_p and CAP_r (that is, thresholds). The slopes a_p and a_r in plotting CAP_p and CAP_r versus the logarithms of $|d_p|$ and $|d_r|$ respectively, indicate the sensitivity of CAP with respect to motion. As the motion components of the stapes are measured on the stapes head in this study, $|d_y|$ represents $|d_p|$, and $|d_x|$ and $|d_z|$ represent $|d_r|$. To simplify the mathematical model, it was assumed that the two rocking-like components had

the same contribution on the CAP, and the total rocking-like component as square-root summation of the two rocking-like components was used

$$|d_r| = \sqrt{|d_x|^2 + |d_z|^2} \,. \tag{4}$$

By defining a ratio $k = |d_r| / |d_p|$ as illustrated in section 2.2, the form of the stapes motion is characterized, whereas $k = 0$ is pure piston, and $k \to \infty$ is pure rocking. With k, the total *CAP* defined in Eqs. (1) – (3) can be represented either with respect to $|d_p|$ or $|d_r|$. That is, $|d_r| = k|d_p|$ is substituted into Eq. (3) for the representation with respect to $|d_p|$, and $|d_p| = |d_r| / k$ is substituted into Eq. (2) for the representation with respect to $|d_r|$.

3. Result

3.1. Schematic Representation of Mathematical Description

As it is assumed that the piston-like component has a larger effect on cochlear activation than the rocking-like component, it is expected that the sensitivity a_p is larger than a_r, and the thresholds $|d_p|_{th}$ are lower than $|d_r|_{th}$. Figure 3 schematically illustrates CAP_p (blue), CAP_r (red), and the total *CAP* (black dot) with respect to $|d_p|$ (figures on the left side) and with resprect to $|d_r|$ (figures on the right side), for small (**A**, $k << 1$, i.e., piston-like dominant), moderate (**B**, $k \approx 1$), and large (**C**, $k >> 1$, i.e., rocking-like dominant) values of k. In the representation with respect to $|d_p|$ (figures on the left side), the CAP_p does not change with values of k, but the CAP_r does change, resulting in a change of the total *CAP*. By contrast, in the representation with respect to $|d_r|$ (figures on the right side), change of the total *CAP* is caused by change of CAP_p. The effects of piston-like and rocking-like motion components on the total *CAP* with different k values were summarized in Fig. 4. In Figs. 3 and 4, the blue points indicate initiation of cochlea activation by the piston-like components, and the red points indicate initiation by the rocking-like components. It should be noted that the slopes a_p and a_r and the thresholds $|d_p|_{th}$ and $|d_r|_{th}$ do not change with k values. Only the representations of CAP_r with respect to $|d_p|$ and CAP_p with respect to $|d_r|$ change with the k value because $|d_r| = k|d_p|$ was used in the representations. If the pure piston-like and pure rocking-like motions of the stapes can be obtained, then the slopes and thresholds can be determined from the curves of CAP_p with respect to $|d_p|$ and CAP_r with respect to $|d_r|$, which do not change with k values. However, in reality stapes motions with our experimental setups always contained both the piston-like and rocking-like components and thus the measured *CAP* contained both CAP_p and CAP_r. The curves of total *CAP* illustrated in Fig. 4 were used to find the slopes and the thresholds in this study.

3.2. Fitting of the Mathematical Description

The slopes a_p and a_r and thresholds $|d_p|_{th}$ and $|d_r|_{th}$, that determine the relation between piston-like and rocking-like displacements of the stapes and the total CAP, were obtained by fitting the mathematical description of the stapes motion-CAP relation shown in Fig. 4. As an initial estimation for the fitting process, an average value of the slopes and thresholds were assumed; however, for the actual fitting, the individual k in all measurements was considered. For the data fitting of the second stage, each of the measurements was also weighted by its measured CAP value.

When the measured CAP values were plotted with respect to the logarithms of measured piston-like and rocking-like components of the stapes motions, a kink in the curve was observed for certain values of k. The kinks corresponded to thresholds and were clearer for measurements with the rocking-like dominant motions due to the relatively large change of the slope. Shifts of the curves by changes in the ratio k were also observed. These results were expected from the schematic representation shown in Fig. 4.

As several different magnitudes of stimulation were applied for each of the stimulation modes, the amplitude ratio k of the rocking-like component to the piston-like component could not be maintained precisely constant. For the second stage of the data fitting, the difference between a measured CAP and a calculated CAP from measured stapes motion components was defined as an error function ε_i in each measurement i

$$\varepsilon_i = CAP_i^M - CAP_i\left(\left|d_p^M\right|_i, \left|d_r^M\right|_i, a_p, a_r, \left|d_p\right|_{th}, \left|d_r\right|_{th}\right), \tag{5}$$

where CAP_i^M was a measured CAP, and CAP_i was calculated from measured stapes motions as defined in Eqs. (1) – (3). Next, the squares of the error functions were summed for the total error E, with each error function ε_i weighted by CAP_i^M

$$E = \sum CAP_i^M \varepsilon_i^2 . \tag{6}$$

The final values for the slopes a_p and a_r and thresholds $|d_p|_{th}$ and $|d_r|_{th}$ were obtained such that the total error E was at its minimum. Regions around the values obtained from the first stage of the data fitting were explored for fine fitting of the second stage.

Table 1 lists the final obtained values of the slopes a_p and a_r and thresholds $|d_p|_{th}$ and $|d_r|_{th}$, for measurements in all six guinea pigs. As the slopes could vary depending on the location of the silver-ball electrode and contact condition between the electrode and cochlear wall, the ratio between the two slopes was considered. Figure 5 shows measured data and the fitted model for GP1, and the results for all other guinea pigs may be found in the Appendix.

The slope a_p was larger than the slope a_r by a factor of about 3.5, and the threshold $\log|d_r|_{th}$ larger than $\log|d_p|_{th}$ by a factor of about 0.3. From these results, the contribution of the piston-like component to the CAP was larger than the contribution of the rocking-like component.

3.3. Error Sources in Measurements

There are three major sources of error: signal-to-noise ratio $\varepsilon_{S/N}$, transversal deviation of the measurement point from the centroid of the stapes footplate ε_{dev}, and error in positioning the stapes footplate in the frame of the test stand ε_{pos}. The first error source was expected to have significant effects for small magnitudes of the measured values (Sim et al. 2010b). As the latter two error sources were already discussed in our previous work (Huber et al. 2008; Sim et al. 2010b), we now consider this error factor quantitatively with respect to *k*.

3.3.1. Signal-to-noise ratio

In our previous work (Sim et al. 2010b), it was shown that the values measured by the LDV systems have a level-independent error, and thus the measured values of small magnitudes contain a relatively small signal-to-noise ratio. Thereby, in fitting the mathematical description of CAP to measured data as described in the previous section, the error function in each measurement was weighted by the amplitude of the measured CAP (Eq. 6).

3.3.2. Error in positioning the stapes footplate in the frame of the test stand

In this study, the stapes was positioned in the frame of the test stand such that the axes of the footplate were parallel and perpendicular to the axes of the test stand, and motions of the stapes measured on the stapes head were decomposed into 3-D components assuming that the axes of the footplate coincide with axes of the frame of the test stand. Therefore, an error in positioning the stapes in the frame of the test stand affects the obtained elementary motion components. Assuming, for simplicity of analysis, that only one rocking-like component d_x exists (i.e., $d_z = 0$ and $d_r = d_x$), and the stapes is positioned in the test frame with an angular position error of θ (Fig. 6), the displacements are

$$d_p^S = d_p^T \cos\theta - d_r^T \sin\theta \tag{7}$$

$$\text{and} \quad d_r^S = d_r^T \cos\theta + d_p^T \sin\theta, \tag{8}$$

where superscript *T* indicates displacements in the frame of the test stand, and superscript *S* indicates true piston-like and rocking-like displacements in the anatomical frame of the stapes. With $k^T = \left|d_r^T\right| / \left|d_p^T\right|$, the error boundaries of the measured displacements are determined by the following equations

$$\varepsilon_{pos,p} = \log\left|d_p^S\right| - \log\left|d_p^T\right| = \log\left(\cos\theta \pm k^T \sin\theta\right) \approx \log\left(1 \pm k^T \theta\right) \tag{9}$$

$$\text{and } \varepsilon_{\mathrm{pos,r}} = \log\left|\mathrm{d_r^S}\right| - \log\left|\mathrm{d_r^T}\right| = \log\left(\cos\theta \pm \sin\theta / \mathrm{k^T}\right) \approx \log\left(1 \pm \theta / \mathrm{k^T}\right). \tag{10}$$

For a piston-like motion, the error is decreasing with decreasing *k*, while for a rocking-like motion, the error is increasing with decreasing *k*.

3.3.3. Deviation of the measurement point from the centroid of the stapes footplate in x and z directions

From the assumption that rocking-like motion components do not produce net volume displacements at the oval window, the piston-like and rocking-like components of the stapes should be obtained with respect to the centroid of the footplate (C in Fig. 1). However, in this study, the piston-like and rocking-like components of the stapes motion were obtained with respect to the measurement point (M in Fig.1), which was located at the stapes head. While the deviation of the measurement point M from the axis orthogonal to the footplate going through the centroid C does not affect the rocking-like components, it affects the calculated piston-like component. With the offsets η+ν and λ+μ in the *x* and *z* directions as shown in Fig.1, the piston-like component at the centroid C of the footplate is calculated as

$$d_p^C = d_p^M - \left(\frac{\eta + \nu}{h} d_x^M + \frac{\lambda + \mu}{h} d_z^M\right), \tag{11}$$

where superscripts *C* and *M* indicate measurement point M and the centroid C of the footplate C, and *h* represents the height of the stapes head from the footplate ($h \approx 1.26$ mm). With $d_z^M = 0$ and $k^M = \left|d_r^M\right| / \left|d_p^M\right|$, Eq. (11) can be expressed as

$$\varepsilon_{dev} = \log\left|d_p^C\right| - \log\left|d_p^M\right| = \log\left(1 \pm \frac{\eta + \nu}{h} k^M\right). \tag{12}$$

From Eq. (12), the effect of this error source on the piston-like component is significant for a large k^M when the rocking-like component is large compared to the piston-like components. In this study, the centroid C of the stapes footplate was accurately obtained with the 3-D shape of the stapes reconstructed from micro-CT imaging. The possible maximum offsets of the measurement point from the centroid of the stapes footplate were 0.094 ± 0.031 mm in the *x*

direction and 0.096 ± 0.019 mm in the z direction from measurements of six guinea pigs. These amounts of the offsets were smaller than 0.4 mm in both x and z directions as assumed in our previous work (Huber et al. 2008).

Assuming an alignment error θ of 5 degrees, and an offset of the measurement point from the centroid of the footplate of 0.1 mm, the CAP and the corresponding errors ε_{dev} and ε_{pos} were calculated. Figure 7 illustrates the error bars for different measurements with different k on GP1. The fit of the model to the measured data can also be seen. Piston-dominant motions show lower errors than do rocking-dominant motions. The error range in the piston direction is larger than in the rocking direction.

4. Discussion

The hypothesis in this study was that both the piston-like and the rocking-like components of the stapes motion contribute to the CAP. Our results indicated that both components activate cochlear responses when they exceed certain thresholds. However, the thresholds as well as the sensitivity of the CAP to the intensity of the motion components are different for the two components. In comparison to the piston-like component, the rocking-like component has a higher threshold (higher by 0.3 nm in the log scale in Table 1) and a lower sensitivity (lower by a factor of 3.47 in Table 1). When the piston-like motion is dominant, then the influence of the rocking component becomes secondary; when the contribution of the piston-like component is low, then the rocking component becomes significant.

Figure 8A displays the total CAP for different motion forms with different k plotted with respect to the absolute value of the piston motion based on the parameters values in Table 1 (a_p/a_r = 3.47 with a_r = 2.2, $\log \left| d_p \right|_{th}$ = 0.57 nm, and $\log \left| d_p \right|_{th}$ = 0.87 nm). This result may be compared to the schematic illustration in Fig. 4A. With k values equal to or less than 1, the CAP is zero below the piston threshold. The CAP increases with the piston sensitivity a_p. The rocking motion contributes to the CAP after the rocking threshold (marked with red dots) is reached. The rocking thresholds depend on the motion form k. With k = 5, the CAP is not zero below the piston threshold because the rocking-like motion activates the CAP (marked with a red circle). Figure 8B points out the contribution of the rocking-like component to the total CAP for different ratios k between rocking-like and piston-like components. The red points indicate the rocking thresholds, and it is clear that the contribution of the rocking increases with increasing k by lowering the threshold. The

maximum percentage of the rocking-like component to the total CAP also increases with increasing k, and it is about 20 % for $k = 1$.

In our experiments, both the piston-like and the rocking-like components were stimulated by the mechanical actuator using a 0.4-ms click (duration of 0.4 ms). Therefore, the identified sensitivities and the thresholds are valid only for this stimulus. However, a harmonic excitation of 1.25 kHz may be comparable to the 0.4-ms click excitation. Earlier measurements (Sim et al. 2010b) of physiological stapes motions on guinea pigs have been carried out with harmonic excitation. The measured physiological motions of the stapes at 1.25 kHz were fed into the mathematical description for calculating the two CAP components. The measured motion at 94 dB SPL delivered a piston displacement of about 120 nm, and the transversal motions of the stapes head were about 40 % leading to $k = 0.4$. Figure 8B indicates the corresponding contribution of rocking to the total CAP of about 13 % as indicated by the brown lines. Here, the maximum contribution is about 16 % due to very large piston displacements.

This study has several limitations. Only a 0.4-ms click signal was used for stimulation, and change in the contribution of the rocking component to the CAP as a function of stimulation frequency was not examined. The two rocking-like components around the long and short axes of the footplate were summarized as only one rocking component, but they could have different influences. Compared to the motion forms found in guinea pigs, human stapes motions show somewhat higher rocking components, especially in the higher frequency range (Hato et al. 2003; Sim et al. 2010a). Therefore, a larger contribution of the rocking-component is expected in human hearing. Particularly when hearing has been restored after reconstruction with passive or active middle-ear prostheses, rocking could be even higher. However, even with these limitations, this study showed contribution of the rocking-like components of the stapes motion to the CAP using controlled mechanical stimulation of the stapes 3-D motion to evoke CAP responses. The contribution of the rocking-like components was also quantified in comparison with the contribution of the piston-like component by introducing a simple mathematical description. More sophisticated models, including measurements on human are planned for the future.

5. Conclusion

In this study, the contributions of the stapes motion components to the CAP have been measured using a distinct mechanical stimulation of 3-D motion patterns of the stapes and were quantified with a simple mathematical description. The rocking-like component of the

stapes motion, which has been considered to have negligible effects on hearing by classical hearing theories, affects the CAP significantly. In the investigations, error bounds have been introduced and evaluated for the measurements taken on guinea pigs. Even assuming maximum error limits, both the piston-like and rocking-like components activate the cochlear responses when they exceed certain thresholds. These thresholds as well as the relation between CAP and intensity of the motion component were different for piston-like and rocking-like components. The threshold was higher and the sensitivity was lower for the rocking-like component than the corresponding values for the piston-like component. The influence of the rocking-like component was secondary in piston-dominant motions of the stapes whereas it may become more significant with low amplitudes of the piston-like component.

The quantitative results of our investigation are based on a very simple mathematical hypothesis. It is expected that more refined descriptions could lead to better insights into the cochlear excitation mechanisms.

ACKNOWLEDGEMENT

This work was supported by SNF Grant No. 31000-120237 and DFG Grant EI 231/4-2.

References

Asai M, Huber A, and Goode R (1999). Analysis of the best site on the stapes footplate for ossicular chain reconstruction. Acta Otolaryngol. (Stockh) 119: 356-361.

Békésy G (1960). Experiments in hearing. McGraw-Hill, New York, NY, USA.

Breuninger C (2008). Zum Übertragungsverhalten des Mittelohrs und der Wirkung der Steigbügelbewegung auf den Hörnerv. PhD. Thesis, University of Stuttgart, Stuttgart, Germany.

Dallos P (1973). The auditory periphery: Biophysics and physiology. New York, Academic Press.

Dodson JM (2001). Efficient finite element methods/ Reduced-order modelling for structural acoustics with applications to transduction. PhD. Thesis, University of Michigan, Ann Arbor, MI.

Decraemer WF and Khanna SM (1999). New insights in the functioning of the middle ear. In: Rosowski JJ. and Merchant SN (Eds.), The Function and Mechanics of Normal, Diseased and Reconstructed Middle Ears. Kugler Publications, The Hague, Netherlands, pp 23-38.

Decraemer WF, de La Rochefoucauld O, Dong W, Khanna SM, Dirckx JJ, and Olson ES (2007). Scala vestibuli pressure and three-dimensional stapes velocity measured in direct succession in gerbil. J. Acoust. Soc. Am. 121 (5): 2774-2791

Eiber A, Breuninger C, Sequeira D, and Huber AM (2007) Mechanical excitation of complex stapes motion in guinea pigs. In: Huber A and Eiber A (Eds.), Middle ear mechanics in research and otology, World Scientific Press, Singapore, pp123-129.

Hato N, Stenfelt S, and Goode RL (2003). Three-dimensional stapes footplate motion in human temporal bones. Audiol Neurootol 8(3): 140-152.

Gundersen T (1971). Prostheses in the ossicular chain: Experimental and clinical studies. University Park Press, Baltimore, MD.

Gyo K, Aritomo H, and Goode RL (1987). Measurement of the ossicular vibration ratio in human temporal bones by use of a video measuring system. Acta-Otolaryngol. 103: 87-95.

Huber AM, Sequeira D, Breuninger C, Eiber A (2008). The effects of complex stapes motion on the response of the cochlea. Otology & Neurotology 29: 1187-1192.

Kirikae I (1960). The Structure and Function of the Middle Ear. The University of Tokyo Press, Tokyo, Japan.

Kolston PJ and Ashmore JF (1996). Finite element micromechanical modelling of the cochlea in three dimensions. J. Acoust. Soc. Am. 99: 455-467.

Lim KM and Steele CR (2002). A three-dimensional nonlinear active cochlea model analyzed by the WKB-numeric method. Hearing Research. 170:190-205.

Linder TE, Furing M, and Huber AM (2003). Round window atresia and its effect on sound transmission. Otol. Neurotol. 24(2): 259-263.

Ombredanne M (1968). Congenital absence of the round window in certain minor aplasias: further cases. Ann. Otolaryngology Chir. Cervicofac. 85: 369-378.

Pozrikidis C (2008) Boundary-integral modeling of cochlear hydrodynamics. J. Fluid and Structures 24: 336-365.

Ravicz ME, Cooper NP, and Rosowski JJ (2008). Gerbil middle-ear sound transmission from 100 Hz to 60 kHz. J. Acoust. Soc. Am. 124: 363-380.

Richards SH (1981). Congenital absence of the round window rerated by cochlea fenestration. Clinical Otolaryngology 6: 265-269.

de La Rochefoucauld O, Decraemer WF, Khanna SM, and Olson ES (2008). Simultaneous measurements of ossicular velocity and intracochlear pressure leading to the cochlear input impedance in gerbil. Journal of the Association for Research in Otolaryngology. 9(2): 161-177.

Schmiedt RA (1979). Basic techniques for measurement of cochlear potentials. In: Beagley HA (ed.), Auditory Investigation: The scientific and technological basis, Oxford University Press, New York, pp. 211-232.

Shera CA and Zweig G (1992). An empirical bound on the compressibility of the cochlea. J. Acoust. Soc. Am. 92(3): 1382-1388.

Sim JH, Chatzimichalis M, Lauxmann M, Röösli C, Eiber A, and Huber AM (2010a). Complex stapes motions in human ears. Journal of the Association for Research in Otolaryngology 11(3): 329-341.

Sim JH, Chatzimichalis M, Lauxmann M, Röösli C, Eiber A, and Huber AM (2010b). Errors in measuring three-dimensional motions of the stapes using a laser Doppler vibrometer system. Hearing Research 270 (1-2): 4-14.

Stenfelt S and Goode RL (2005). Transmission properties of bone conducted sound: measurements in cadaver heads. J. Acoust. Soc. Am. 118: 2373-2391.

Voss SE, Rosowsky JJ, Merchant SN, and Peake WT (2000). Acoustic responses of the human middle ear. Hearing Research 150: 43-69.**Appendix** Fitting measured data to the mathematical model in all guinea pigs.

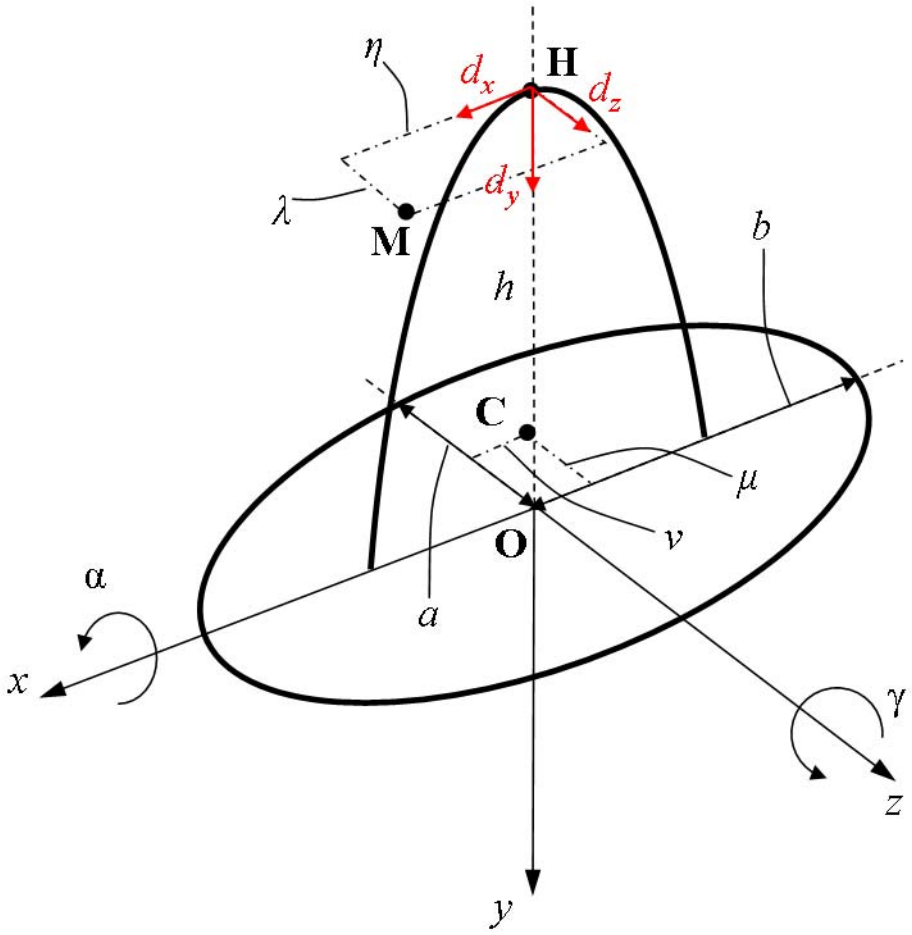

Fig. 1. Definition of axes, dimensions of the stapes, significant points, and displacements at the stapes head. d_x (= $h\gamma$) represents the rocking-like displacement around the short axis (z-axis) of the footplate, d_y the piston-like displacement, and d_z (= $-h\alpha$) the rocking-like displacement around the long axis (x-axis) of the footplate.

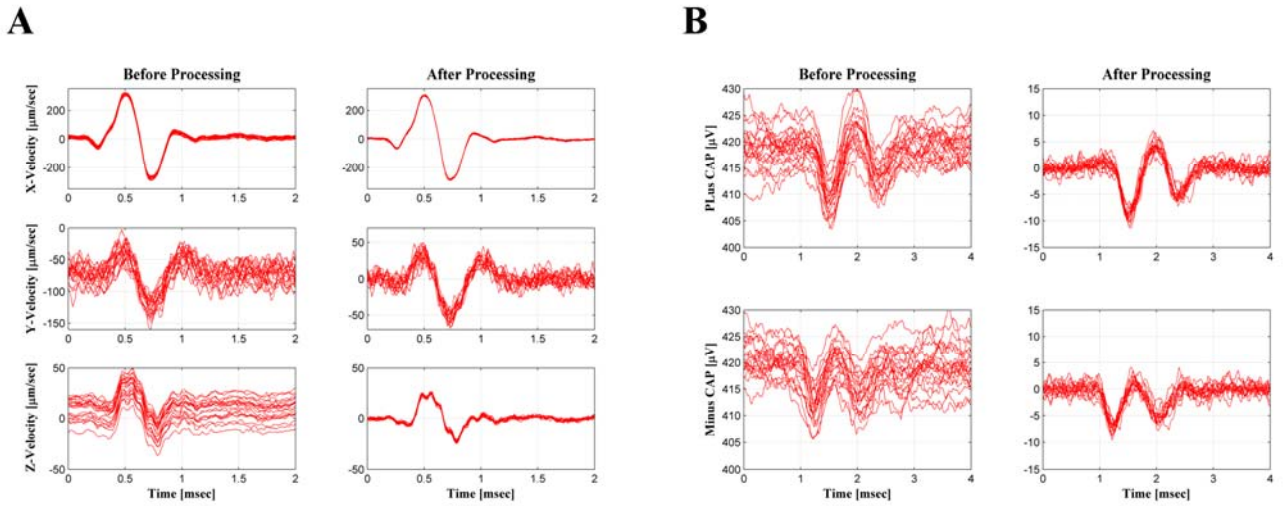

Fig. 2. Elimination of noise and offset: **A** in the measured stapes motions and **B** in measured CAP for *x*-dominant motion of the stapes. After constant and linear trends were eliminated with the 'detrend' function in Matlab and data sets showing large deviations from other data were excluded, the measurements were averaged for the final measured values. 'Plus' and 'Minus' indicate repeated measurements with the two opposite directions of the stimuli, which were made to confirm the firm contact between the stapes and the actuator needle at their interface (i.e., no relative motion and no initial load on the stapes as well).

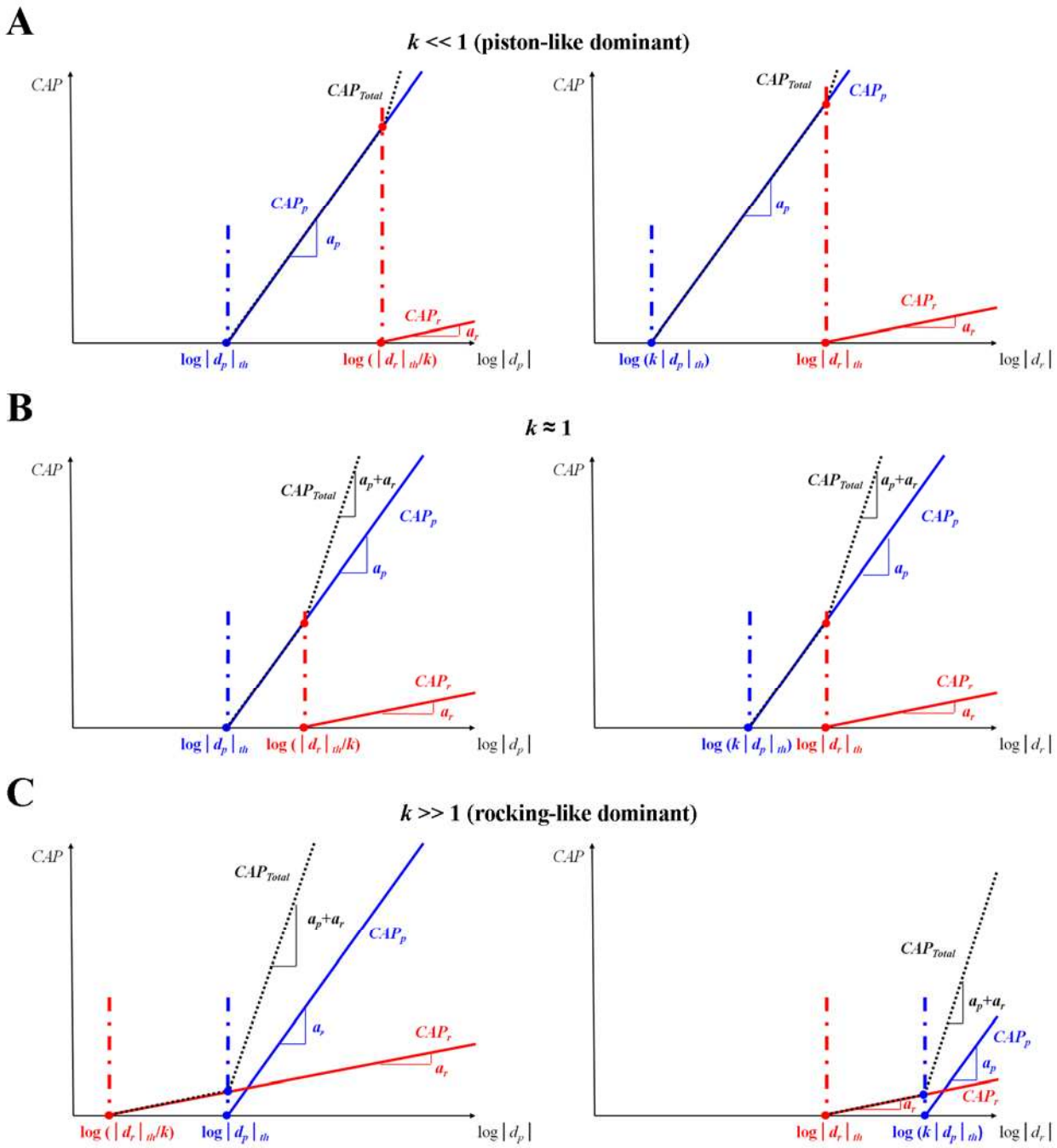

Fig. 3. Schematic representation of CAP_p, CAP_r, and total CAP with respect to the logarithm of the piston-like displacement $\log \left| d_p \right|$ (left) and with respect to the logarithm of the rocking-like displacement $\log \left| d_r \right|$ (right), **A** for $k << 1$, piston-like dominant), **B** for $k \approx 1$, and **C** for $k >> 1$ (rocking-like dominant). Red dots indicate kink points where CAP_r is activated by the rocking-like component (i.e., threshold of CAP_r), and blue dots indicate kink points where CAP_p is activated by the piston-like component (i.e., threshold of CAP_p).

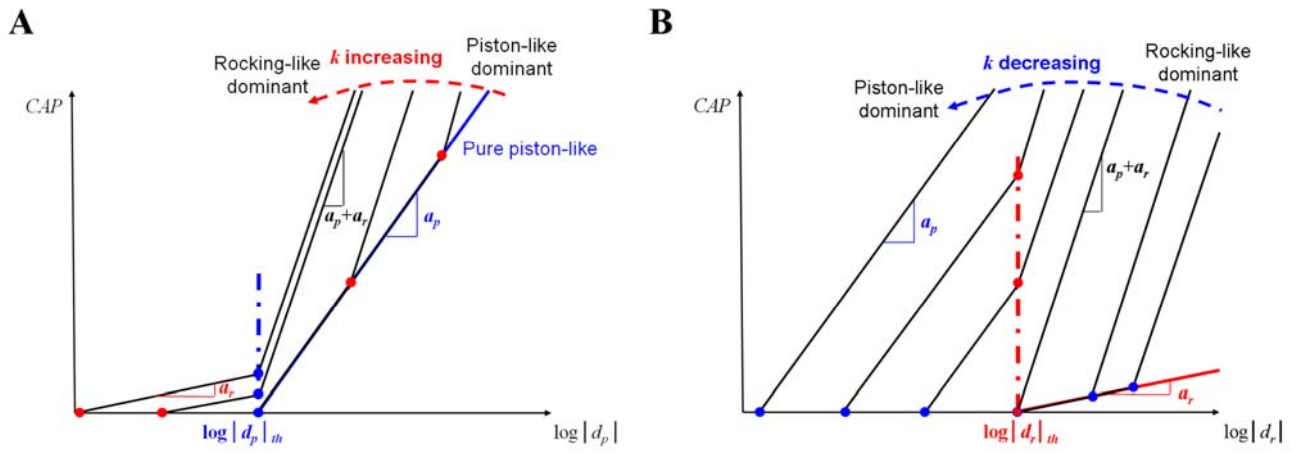

Fig. 4. Schematic representation of the total CAP for different amplitudes ratio k of the piston-like component $|d_p|$ to the rocking-like component $|d_r|$ of stapes motions, with respect to logarithm of the piston-like displacement $\log|d_p|$ (left) and with respect to logarithm of the rocking-like displacement $\log|d_r|$ (right). Red dots indicate kink points where CAP_r is activated by the rocking-like component, and blue dots indicate kink points where CAP_p is activated by the piston-like component.

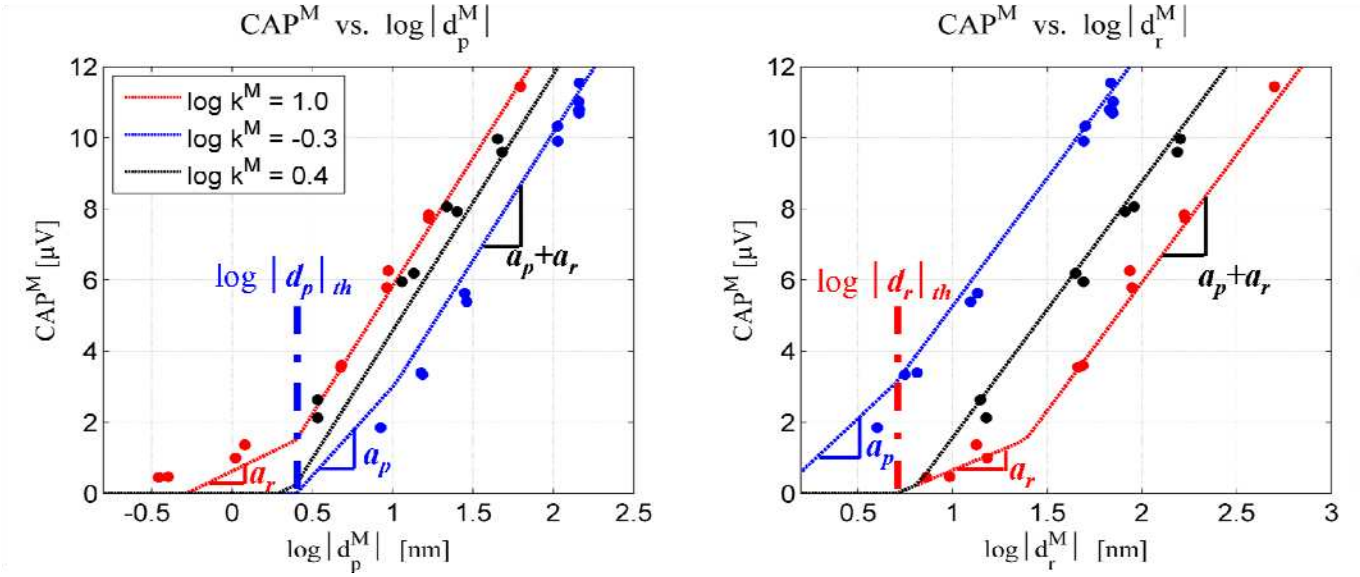

Fig. 5. Fitting of the mathematical description of CAP (solid lines) to measured data (dots) in GP1. Relation between the piston-like component and CAP (left) and relation between the rocking-like component and CAP (right).

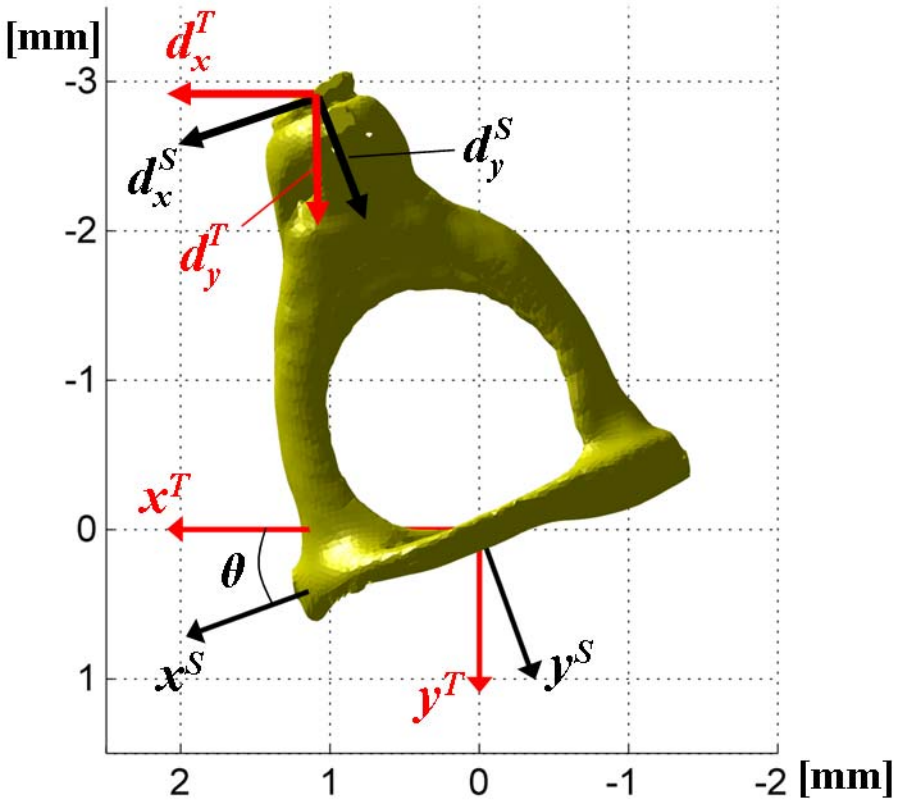

Fig. 6. Error in positioning the stapes footplate in the frame of the test stand. x^T and y^T indicate axes of the test stand frame, x^S and y^S indicate axes of the anatomical frame of the stapes, and θ indicates alignment error between the two frames.

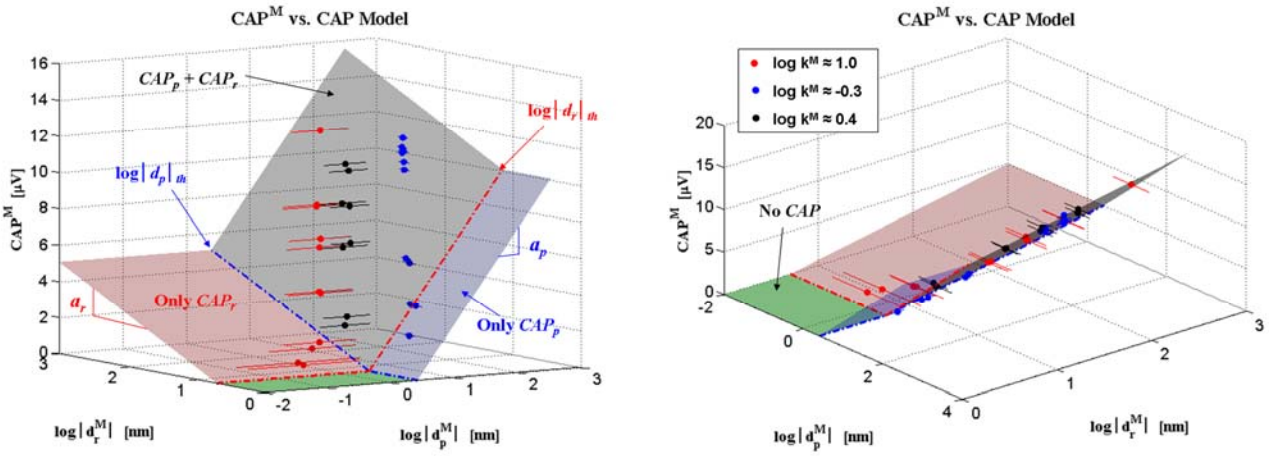

Fig. 7. Relation between the stapes motion components and CAP and possible error range (GP1) from two different perspective views. A line at each measurement point represents the range of maximum possible error due to error in positioning the stapes in the frame of the test stand and deviation of the measurement point from the centroid of the stapes footplate.

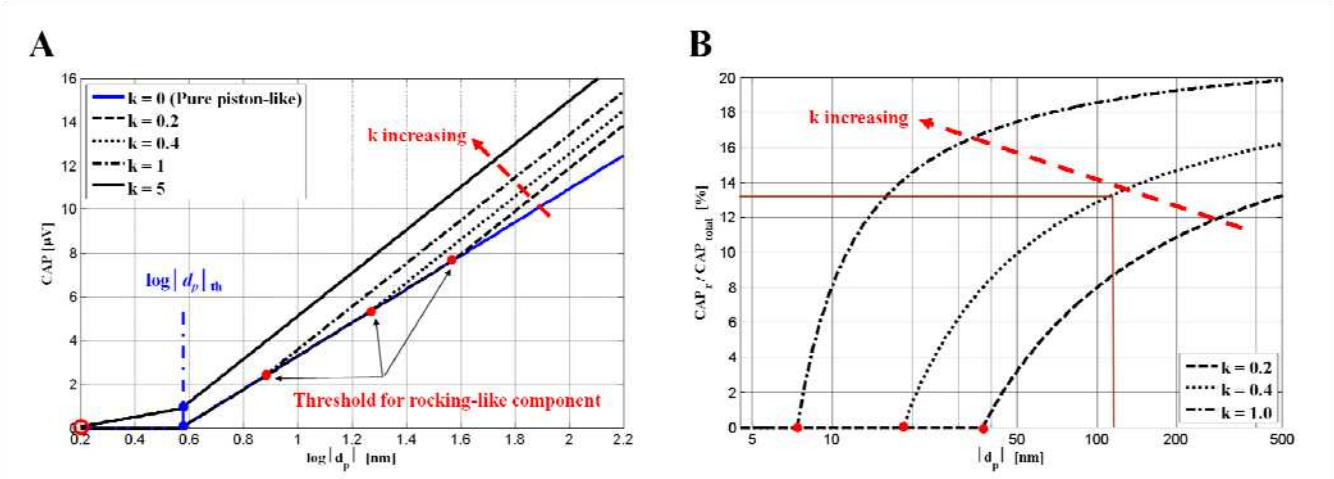

Fig. 8. Contribution of the rocking-like component to CAP. **A** Change of the total CAP and **B** relative contribution of the rocking component to the total CAP with different ratios between the rocking-like and piston-like components. Red dots (for k≤1) and circle (for *k*=5) indicate the points where CAP_r is activated by the rocking-like component (See Fig. 3).

Fig. A1

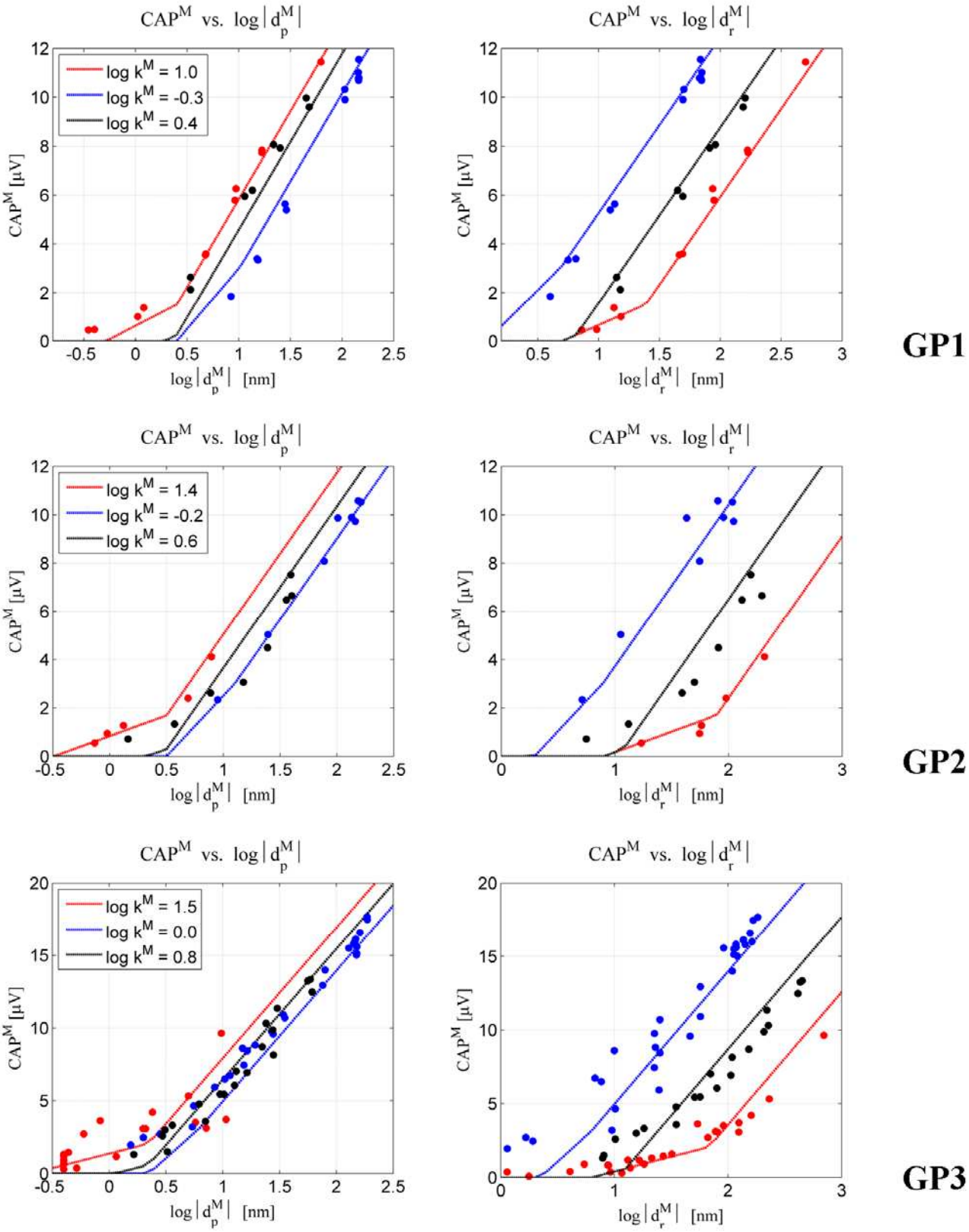

Fig. A1. Fitting the mathematical description of CAP to measured data in all guinea pigs.

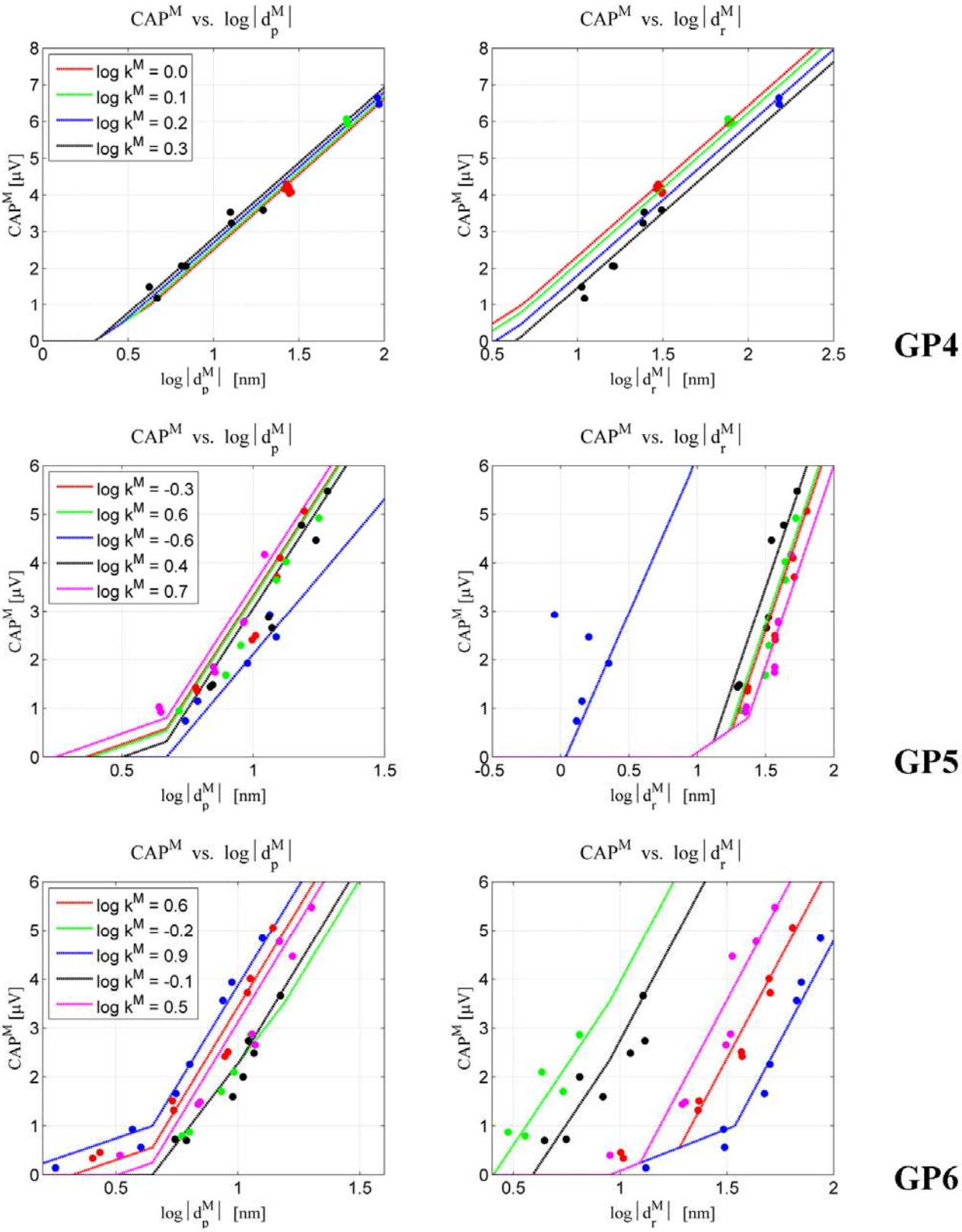

Fig. A1 (Continued)

Table 1. Slopes and thresholds in a mathematical model of CAP as a linear combination of the logarithms of the piston-like and rocking-like components. As the slopes a_p and a_r could vary depending on the location of the silver-ball electrode and contact condition between the electrode and cochlear wall, the ratio between the two slopes was used.

	a_p / a_r	$\log \lvert d_p \rvert_{th}$ [nm]	$\log \lvert d_r \rvert_{th}$ [nm]
GP1	2.3	0.40	0.70
GP2	3.8	0.85	1.00
GP3	3.8	0.35	0.80
GP4	2.7	0.30	0.70
GP5	3.2	0.70	0.90
GP6	3.8	0.65	0.95
Mean	3.47	0.57	0.87
STD	0.50	0.24	0.12